JOURNAL OF CATALYSIS 128, 198–209 (1991)

A TPD and XPS Investigation of Palladium on Modified Alumina Supports Used for the Catalytic Decomposition of Methanol

D. T. WICKHAM, B. W. LOGSDON, AND S. W. COWLEY

Department of Chemistry and Geochemistry, Colorado School of Mines, Golden, Colorado 80401

AND C. D. BUTLER

Rocky Mountain Laboratories, 602 Park Point Drive, Suite 101, Golden, Colorado 80401

Received October 31, 1989; revised September 24, 1990

A series of modified palladium catalysts on alumina supports previously have been prepared and evaluated for selectivity, activity, and thermal stability in decomposing methanol into CO and H_2. In this investigation the modified palladium catalysts are characterized by X ray photoelectron spectroscopy (XPS) and CO and NH_3 temperature-programmed desorption (TPD). Average particle sizes of the palladium crystallites were also determined using chemisorption techniques. The XPS results indicate that the lithium-modified catalyst, which deactivated substantially during methanol decomposition testing, exhibited a significant build-up of carbon on the catalyst surface, while a similar accumulation was not observed for the lanthanum-modified catalyst under identical conditions. The CO TPD results show that the lithium-, sodium-, and barium-modified catalysts, which deactivate during methanol decomposition testing, produce a much greater amount of CO_2 relative to the amount of CO desorbed than do the potassium-, rubidium-, cesium-, and lanthanum-modified and the unmodified catalysts, which do not deactivate considerably under identical conditions. Ammonia TPD and chemisorption results indicate that no correlation exists between support acidity or particle size and the degree of CO dissociation. Finally, a correlation between the charge density of the modifier and the degree of CO disproportionation is presented which fits for all cases except one. This appears to support an electrostatic model for the promotion of CO bond cleavage by the alkali modifier.

INTRODUCTION

Previous reports (*1–4*) have shown that the efficiency of methanol when used as an automotive fuel can be improved by approximately 20% if, prior to combustion, it is decomposed into carbon monoxide and hydrogen as shown below:

$$CH_3OH \longrightarrow CO + 2\,H_2. \qquad (1)$$

Cowley and Gebhard have found that an alumina supported palladium catalyst can catalyze Eq. (1) with high selectivity if basic modifiers are added to the catalyst in order to decrease the acidity of the support (*5*). However, these modifiers also have a significant effect upon the thermal stability and activity of the metal function (*6, 7*). This is illustrated in Table 1 where results of methanol decomposition experiments from Ref. (*6*) are tabulated. The modifier effects can be summarized by the following observations. First, the addition of the modifier to the 3 wt% palladium catalysts increased the initial selectivity for H_2 and CO. Second, the initial activity of each modified catalyst is lower than that of the unmodified catalyst. A more detailed discussion of these points is found in Ref. (*6*). The third point, which is the primary focus of this investigation, is that the catalysts modified with Li, Na, and Ba lose greater than 60% of their original activity after the methanol decomposition reaction is carried out at 500°C, while the catalysts modified with K, Rb, Cs, and La lose less than 30% of their original activity when exposed to identical reaction conditions. Since Cowley and Gebhard (*5*) have shown that the behavior of the lithium- and lanthanum-modified catalysts is not affected by

0021-9517/91 $3.00

TABLE 1

Results of Catalyst Evaluations for Determining Activity, Selectivity, and Thermal Stability for the Modified Palladium Catalysts Along with an Unmodified Palladium Catalyst

Catalyst modifier	Initial activity	Select. CO/hyd.	Final activity	Activity ratio
Unmodified	100	91	100	1.0
Lanthanum	85	100	79	0.92
Cesium	55	95	51	0.93
Lithium	82	99	2	0.03
Barium	81	94	31	0.38
Sodium	77	99	28	0.37
Potassium	86	97	63	0.73
Rubidium	66	99	55	0.84

Note. Space velocity = 1.9 g CH_3OH (g cat h)$^{-1}$. Initial activity = 100 − % CH_3OH in products at the initial 300°C temperature. Selectivity for CO and H_2 = (%CO + %H_2)/(100 − % CH_3OH) at the initial 300°C temperature. Final activity = Activity at 300°C after temperature was maintained at 500°C for 2 h. Activity ratio = final activity/initial activity.

the presence or absence of the chloride ion, this investigation focuses only on the effect of the metals used for the catalyst modification.

Although much work (*8–17*) has focused on the effect of the alkali modifiers in both single crystal and supported metal studies, the exact role of the modifier in reactions such as CO disproportionation is still not known. The two models which have been proposed to account for these effects are based on the migration of the modifier onto the surface of the active metal. In one model (*8–12*), the modifier promotes C–O bond cleavage by promoting the metal's donation of electrons into the C–O antibonding orbitals. In the other model (*13–17*), a direct electrostatic interaction between the positively charged modifier and the oxygen of an adsorbed CO molecule accounts for the decrease in the C–O bond strength.

In this investigation, four of the supported palladium catalysts listed in Table 1 have been characterized by X ray photoelectron spectroscopy (XPS). In addition, all of the catalysts listed in Table 1 were characterized by CO temperature-programmed desorption (TPD), NH_3 TPD, and chemisorption techniques. The results of these experiments were used to study the role of the modifier in the catalyst deactivation.

EXPERIMENTAL PROCEDURE

Catalyst Preparation and Testing Apparatus

The preparation of the modified palladium catalysts has been described previously (*5, 6*). Briefly, nitrate salt solutions were used to impregnate γ-alumina, by Alpha Products (99% Al_2O_3) with the specified modifier using incipient wetness. The modified support was calcined at 500°C for 12 h, and then the material was impregnated with palladium using a solution of palladium (II) chloride. The catalyst was dried and then calcined again at 500°C before use. All catalysts consisted of nominal 3% (by weight) palladium on a γ-alumina support. This concentration of palladium was chosen in order to facilitate subsequent characterization of the catalysts. Modifier additions were 3.5% by weight Li_2O, or 5.0% by weight Na_2O, K_2O, Rb_2O, Cs_2O, BaO, or La_2O_3.

Catalyst Characterization by XPS

XPS characterizations were performed on the unmodified, the lanthanum-, lithium-,

and cesium-modified catalysts at three stages: (1) after the final calcination step of the catalyst preparation, (2) after reduction in hydrogen, and (3) after methanol decomposition testing.

The reduced catalysts were prepared by placing a catalyst sample in a catalytic reactor (described in Ref. (*5*)) and exposing it to a hydrogen flow of 30 cm^3/min at 400°C for 2 h. The catalysts were then cooled to less than 40°C in the helium flow and then removed from the reactor.

The tested catalysts were first reduced at 400°C for 2 h as above. After sweeping the hydrogen from the system with helium and lowering the temperature to 300°C, methanol vapor was introduced at a space velocity of 1.9 g methanol/g catalyst h. The catalyst temperature was held at 300°C for 1.5 h, raised to 500°C and held for 2 h, and then lowered to 300°C for 1.0 h. At the conclusion of the test, the methanol flow was discontinued and the catalysts were cooled to less than 40°C in helium.

No further preparation of the catalyst was performed once the particles were removed from the reactor. The XPS analyses were performed on a Surface Science SSX-100 XPS instrument equipped with a resistive anode detector and an aluminum K alpha source emitting 1486 eV x-rays. The pass energy of the concentric hemispherical analyzer was 150 eV nominally. Quantification was accomplished after correction for the total transmission function, which includes the instrument transmission and correction for the energy dependent escape depth function. Two references were used to calculate the total work function: the carbon 1*s* peak at 284.6 eV and the Al 2*p* peak of Al_2O_3 at 74.2 eV (*18, 19*). For this series, these values agreed to within 0.1 eV. Depth profiles also were performed on the tested forms of the lithium- and lanthanum-modified catalysts. These profiles were accomplished by alternately performing an XPS scan and then exposing the surface to a rastered beam of Ar^+ ions, accelerated by a potential of 2 kV for an interval of 30 s. Both depth profiles were performed using identical ion fluxes.

CO Temperature-Programmed Desorption

The CO TPD apparatus consisted of a gas manifold through which either hydrogen or helium could be passed at a controlled flow rate. A gas sampling valve was attached to the manifold so that reproducible pulses of CO could be injected into the carrier stream. The gas stream was passed through a quartz cell which contained the catalyst bed and then into a quadrupole mass spectrometer (Leybold Heraeus—IQ 200) by way of a low pressure buffer chamber. The quartz cell was enclosed by a tube furnace, which was controlled by a linear temperature programmer. Ultra high purity hydrogen and helium (99.999%) and reagent grade CO (99.99% purity) were supplied by Scientific Gas Products. Helium was passed through a heated gas purifier from Supelco Inc. and an Oxyclear unit from Matheson Gas Products, while hydrogen was passed through a Deoxy catalyst from Englehard Corp. and a scrubber containing Union Carbide 4A molecular sieve and indicating Drieright from W. A. Hammond Drierite Company. Carbon monoxide was passed through a Deoxo oxygen remover provided by Scientific Gas Products.

Approximately 0.3 g of catalyst was placed in the reactor tube. It was then reduced in a 30 cm^3/min H_2 flow at 400 or 500°C for 2 h and cooled to 25°C in helium. The catalyst surface was then saturated with CO by injecting pulses of CO into the carrier stream. Following CO adsorption, the He carrier flow was adjusted to 80 ml/min and the catalyst temperature was increased at a constant rate of 25°C/min. The mass spectrum was recorded at 10° intervals until a final temperature of 600°C was achieved.

NH_3 Temperature-Programmed Desorption

Three modified alumina supports and one unmodified alumina support were prepared

and analyzed for total acidity by ammonia temperature-programmed desorption. The weight percent additions of the modifiers were 3.5% Li_2O, 5% La_2O_3, and 5% Cs_2O. Standard impregnation procedures using the nitrate salt of each modifier were used. In addition, 9.6 wt% chloride was added to each support in order to simulate the chloride concentration on the palladium catalysts as a result of using palladium chloride in their preparation.

The apparatus used in these experiments is similar to the CO TPD apparatus described above. The primary difference in this system is that a thermal conductivity detector was used instead of the mass spectrometer for NH_3 detection. In addition, as the sample stream exited the detector, the ammonia was collected in a series of two acid scrubbers each containing 10.0 ml of a standardized, 0.05 *N*, sulfuric acid solution.

Approximately 0.5 g of each support was placed in the reactor tube and dried in a 30 cm^3/min helium flow for 1 h at 600°C. The catalyst temperature was lowered to 175°C, and the carrier flow was replaced by a flow of anhydrous ammonia (from Scientific Gas Products) for 30 min. After the 30-min adsorption, the gas flow was switched from ammonia to helium, and the excess ammonia was swept from the support until a constant signal was obtained on the chart recorder. The temperature then was increased at a constant rate of 20°C/min and the detector output recorded until a final temperature of 500°C was reached. At the conclusion of the run, the acid solutions were titrated with the standard sodium hydroxide solution to a methyl-red end point. The amount of ammonia desorbed during the run was determined directly from the amount of sulfuric acid consumed in the titration.

Chemisorption Studies

The concentration of surface Pd atoms was determined by three methods: H_2–O_2 titration, H_2 chemisorption, and CO chemisorption. The procedure followed was that used by Benson *et al.* (*20*). The bulk palladium concentration determined by atomic absorption spectroscopy was used to calculate the Pd crystallite size.

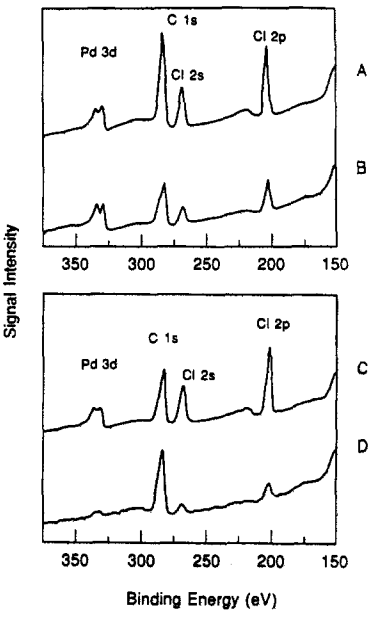

FIG. 1. XPS survey scans of the reduced (A) and tested (B) forms of the lanthanum-modified palladium catalyst and the reduced (C) and tested (D) forms of the lithium-modified palladium catalysts.

RESULTS AND DISCUSSION

XPS: Surface Palladium Content

Figure 1 shows XPS scans between 150 and 400 eV for the reduced and tested stages of the lanthanum- and lithium-modified catalysts. The palladium peaks are labeled as are peaks for carbon and chlorine. The presence of chlorine is attributed to the use of palladium chloride in the catalyst preparation. These XPS scans show that a severe loss in intensity in the Pd 3*d* peaks occurs for the lithium-modified catalyst between the reduced and tested stages. However, the loss in intensity is not significant for the lanthanum-modified catalyst. The results for the cesium and unmodified catalyst were similar to those observed for the lanthanum-modified catalyst.

The surface composition of each stage of

TABLE 2

Elemental Surface Composition of the Calcined, Reduced, and Tested Stages of the Unmodified and of the Lanthanum-, Lithium-, and Cesium-Modified Palladium Catalysts Determined by XPS

Catalyst	Surface concentration (atomic%)					
	Pd	O	Al	C	Cl	Cs
Unmodified						
calcined	0.76	56.5	29.7	11.4	1.0	
reduced	0.76	60.3	30.9	6.5	1.3	
tested	0.23	62.5	31.2	5.7	0.2	
Lithium-modified						
calcined	0.46	60.0	30.6	6.3	2.5	
reduced	0.23	61.0	30.5	5.9	2.4	
tested	0.05	62.7	29.8	6.6	0.6	
Lanthanum-modified						
calcined	0.53	56.8	29.9	10.6	2.2	
reduced	0.26	58.1	29.6	9.5	2.5	
tested	0.30	61.4	31.3	5.5	1.3	
Cesium-modified						
calcined	0.47	50.6	38.5	7.5	1.0	1.7
reduced	0.23	52.0	38.2	6.9	0.9	1.9
tested	0.24	49.5	42.8	4.4	0.5	2.6

the four catalysts was calculated from the XPS peak areas and the results are presented in Table 2. These results also show that the effect of the modifier is significant with respect to the amount of surface palladium detected following the testing sequence. The lanthanum- and cesium-modified catalysts show no significant changes in palladium concentration between the reduced and tested stages. However, the lithium-modified catalyst does not follow this trend and exhibits a significant loss in surface palladium, decreasing from 0.23% after reduction to 0.05% after testing. The unmodified catalyst also shows some loss in surface palladium, although the value of 0.23% after testing is similar to the values observed for the cesium- and lanthanum-modified catalysts.

Analyses for total palladium were performed by atomic absorption spectroscopy. These determinations showed that no significant change in bulk palladium concentration occurred during the testing cycle for any of the catalysts. Therefore, it can be concluded that the changes in palladium content as shown by XPS reflect changes in the concentration of surface palladium only.

Three additional observations from Table 2 deserve comment. First, in all cases the chlorine concentration decreases following testing. This is likely due to the formation of HCl which is then removed by water that forms in small quantities during the testing sequence. The second observation is that the ratios of oxygen to aluminum for the unmodified and the lithium- and lanthanum-modified catalysts exceed the expected value of 1.5. This may be due to the formation of AlOOH on the surface of the support (*21*); in addition, the formation of palladium and modifier oxides also would contribute to the high O : Al ratio. The reason for the lower value for the cesium-modified catalyst is not clear. The third observation is that lanthanum and lithium were not detected for the catalysts modified with these elements. Lithium is relatively insensitive to XPS, and therefore, it is not surprising that this element was not observed. However, lantha-

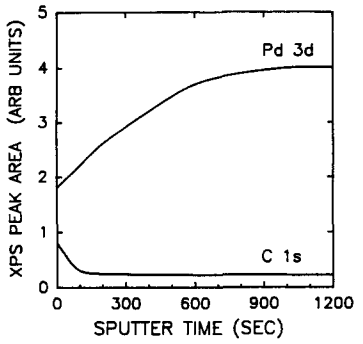

FIG. 2. XPS measurement of the Pd 3*d* and C 1*s* peak areas as a function of sputter time for the tested form of the lanthanum-modified palladium catalyst.

num should have been detected; additional investigation is needed in order to explain this observation.

XPS Depth Profiles

The depth profiles monitoring the Pd 3*d* and the C 1*s* electron signals of the tested forms of the lanthanum- and lithium-modified catalysts are summarized in Figs. 2 and 3 respectively. These figures show the relative peak areas of the two elements as a function of sputter time. Comparison of these figures show that the ratio of the carbon to the palladium signal is much greater near the catalyst surface (shorter sputter times) for the lithium-modified catalyst compared to that observed for the lanthanum-modified catalyst. As the sputter time increases, the relative ratios are similar for two catalysts. This implies that the palladium metal on tested form of the lithium-modified catalyst is covered with a thicker carbon layer than is found on the same form of the lanthanum-modified catalyst. This conclusion is consistent with the data presented in Fig. 1 and Table 2, and likely accounts for the significant deactivation of the lithium-modified catalyst observed in Table 1. After deactivation, a lithium-modified catalyst was reoxidized in air at 500°C in the reactor tube and again exposed to methanol. The reoxidized catalyst regained approximately 80% of the original activity of the catalyst. This observation is consistent with the conclusion that coking was the cause of deactivation of the lithium-modified catalyst.

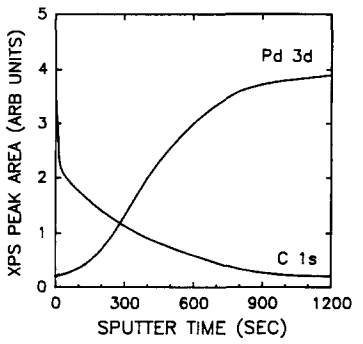

FIG. 3. XPS measurement of the Pd 3*d* and C 1*s* peak areas as a function of sputter time for the tested form of the lithium-modified palladium catalyst.

CO Temperature-Programmed Desorption

The thermal desorption profiles for the modified palladium catalysts are shown in Figs. 4 and 5. The profiles for the cesium-, potassium-, rubidium-, and lanthanum-modified catalysts are shown in Fig. 4, while those for the sodium-, barium-, and lithium-modified catalysts are shown in Fig. 5. These figures show that CO_2 formation occurs in addition to CO desorption during the temperature ramp and that the relative amounts of CO and CO_2 are greatly affected by the particular modifier present.

The formation of CO_2 is assumed to result from the disproportionation of CO as shown below:

$$2\,CO(a) \longrightarrow C(a) + CO_2. \qquad (2)$$

Equation (2) shows that for every molecule of CO_2 formed, one molecule of carbon is generated which remains on the catalyst surface. The oxidation of CO is not believed to contribute significantly to the production of CO_2 because the prior reduction in H_2 should have removed any reactive oxygen on the catalyst surface. Thus, the relative areas under the CO and CO_2 peaks reflect the tendency of each of the modified cata-

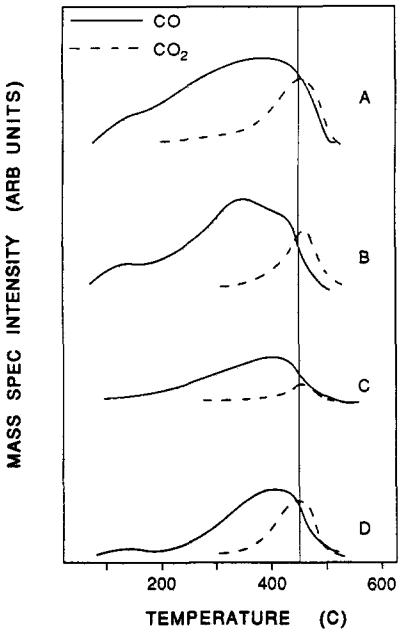

FIG. 4. CO TPD profiles of the cesium-modified (A), the potassium-modified (B), the rubidium-modified (C), and the lanthanum-modified (D) catalysts following reduction at 500°C.

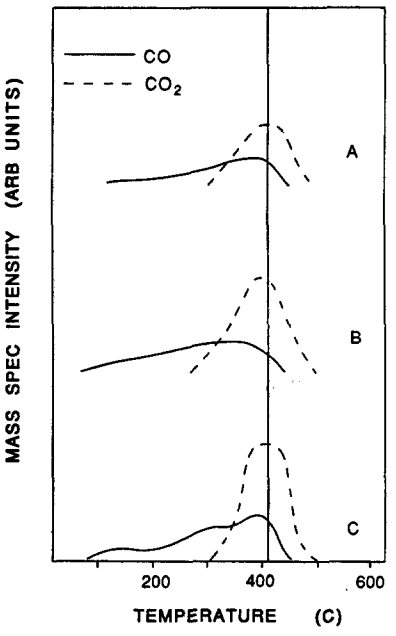

FIG. 5. CO TPD profiles of the sodium-modified (A), the barium-modified (B), and the lithium-modified (C) catalysts following reduction at 500°C.

TABLE 3

Fraction CO Desorbed [CO/(CO + CO_2)]

Catalyst modifier	Fraction CO Desorbed [CO/(CO + CO_2)] Reduction temperature (°C)	
	400	500
Unmodified	—	0.60
Lithium	0.30	0.36
Sodium	0.36	0.33
Potassium	0.70	0.73
Rubidium	0.64	0.69
Cesium	0.69	0.70
Barium	0.30	0.38
Lanthanum	0.66	0.65

lysts to promote Eq. (2) and, therefore, CO bond cleavage.

The difference between the profiles shown in Figs. 4 and 5 is apparent from an examination of the relative heights of the CO and CO_2 peaks for each catalyst. The CO_2 peak maximum is less intense than the CO peak maximum for the catalysts shown in Fig. 4, while the reverse is true for the catalysts shown in Fig. 5. These results suggest that the sodium-, barium-, and lithium-modified catalysts promote CO disproportionation, and therefore, CO bond cleavage relative to the lanthanum-, cesium-, rubidium-, and potassium-modified catalysts. The TPD profile for the unmodified catalyst was similar to those shown in Fig. 4.

CO temperature-programmed desorption experiments also were performed on the catalysts after reduction at 400°C. The relative intensities of the CO and CO_2 profiles were similar to those following the 500°C reduction.

The peak areas in Figs. 4 and 5 and those where reduction was performed at 400°C were integrated and the fraction CO desorbed [CO/(CO + CO_2)] was calculated for each temperature-programmed desorption experiment; these values are listed in Table 3. The result for the unmodified catalyst is also included for the case where reduction

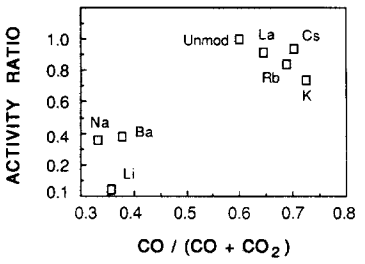

FIG. 6. Plot of activity ratio for catalysts during methanol decomposition testing against fractional CO area [CO/(CO + CO_2)] from CO TPD.

was performed at 500°C. This table reaffirms the earlier observations that the lithium-, sodium-, and barium-modified catalysts greatly promote Eq. (2), as evidenced by lower values of fraction CO desorbed relative to the other catalysts. The data from this table also show that the catalyst reduction temperature does not have a significant effect upon the extent to which the disproportionation reaction occurs.

Since CO is a product molecule in the methanol decomposition reaction, Eq. (1), the above data suggest that deactivation due to carbon deposition from Eq. (2) may occur to a greater extent on the lithium-, sodium-, and barium-modified catalysts than on the other catalysts when the reaction is conducted at temperatures greater than 400°C. This suggestion is supported by the methanol decomposition testing results of Table 1 which show that the lithium-, sodium-, and barium-modified catalysts deactivate to a much greater extent than do the other catalysts following testing at 500°C.

The correlation between the methanol decomposition testing and the CO TPD results is clearly shown in Fig. 6. Those catalysts which had an activity ratio of less than 0.4 during the methanol decomposition reaction sequence (see Table 1) also exhibited values of less than 0.4 for fraction CO desorbed during the CO TPD experiments (see Table 2). By contrast, the catalysts with higher activity ratios also had greater values for faction CO desorbed.

Rieck and Bell have studied the addition of lanthanum (*22*) and alkali metals (*23*) to silica-supported palladium catalysts. They found that the addition of lanthanum and all alkali metals (after a 400°C reduction) promoted the CO disproportionation reaction relative to the unmodified silica-supported palladium catalyst. Although these results appear to differ from those presented here, it is well known that the catalyst support can affect the behavior of the catalyst significantly (*24, 25*). As the work of Rieck and Bell involved silica-supported rather than alumina-supported catalysts, it is not surprising that their results are different from those obtained in this study.

Ammonia TPD Results

Figure 7 shows the ammonia desorption profiles of the unmodified support along with those of the supports modified with lanthanum, lithium, and cesium as a function of support temperature. The three modified supports all show one desorption maximum between 270 and 300°C. The profile for the unmodified support, Fig. 7d, shows a similar maximum at approximately 300°C, and also has a shoulder centered at approximately 450°C. The quantities of ammonia desorbed decreased in the following order (all values in moles NH_3 per gram support): unmodified—0.13; lanthanum-modified—0.11; lithium-modified—0.10; and cesium-modified—0.047.

Although support acidity has been shown to have a substantial effect upon catalyst activity and selectivity (*26–28*), the above

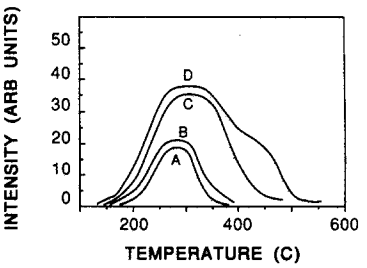

FIG. 7. Ammonia TPD profiles for alumina supports modified with cesium (A), lithium (B), and lanthanum (C), in addition to an unmodified alumina (D) support.

data suggest that this factor does not exclusively govern the extent to which the catalysts studied here promote Eq. (2). As discussed above, the CO TPD data indicate that the lithium-modified palladium catalyst promotes Eq. (2) relative to the lanthanum- and cesium-modified and unmodified catalysts as evidenced by lower values of fraction CO desorbed (see Table 3). If support acidity played an important role in this behavior, then a significant difference would be expected between the acidity of the lithium-modified support and the acidities of the other three supports evaluated in this study. However, the data show that the acidity of the lithium-modified support is not substantially different from the acidities of the other supports and, in fact, lies approximately in the middle of the range of acidities obtained. In addition, the acidities of the cesium- and lanthanum-modified supports are at opposite ends of the range obtained while the CO TPD data show that the cesium- and lanthanum-modified palladium catalysts exhibit similar behavior with regard to the promotion of Eq. (2). Therefore, it can be concluded that for the catalysts and supports studied here, no apparent correlation exists between the acidity of the catalyst support and the tendency of the corresponding palladium catalyst to promote Eq. (2).

Particle Size Determination

The average size of the palladium crystallites of each of the tested catalysts has been determined by chemisorption and the data are presented in Table 4. Since some of the alkali modifier may have migrated onto the palladium surface, the values presented here likely represent upper limits. However, these results agree qualitatively with average palladium particle size determinations from x-ray diffraction line broadening studies (*29*), and therefore the assumption can be made that the modifier has not affected the particle size determinations significantly.

Although smaller palladium particle sizes have been suggested to promote CO disproportionation on silica-supported catalysts (*30, 31*), it does not appear that this factor predominates on the alumina-supported catalysts studied here. Table 4 shows that the catalysts with the smallest particle diameters are the unmodified and the potassium-, cesium-, and rubidium-modified catalysts. However, Table 1 shows that these catalysts do not deactivate substantially, and Table 3 shows that they have relatively high values for fraction CO desorbed and therefore do not promote Eq. (2) relative to the others studied. Additionally, the catalyst with the largest particle diameter in Table 4 is the sodium-modified catalyst. Table 1 shows that this catalyst undergoes a significant deactivation and Table 3 shows that it has a low value for fraction CO desorbed and therefore promotes Eq. (2) relative to the other catalysts. The data therefore suggest that for the catalysts studied here, the importance of particle size in the promotion of Eq. (2) is outweighed by the presence of a particular modifier.

TABLE 4

Average Particle Size Determined by H_2–O_2 Titration, H_2 and CO Chemisorption

Catalyst modifier	Average Particle Diameter (Angstroms)		
	H_2–O_2 titration	H_2 chemisorption	CO chemisorption
Unmodified	26	24	27
Lanthanum	74	88	66
Cesium	49	39	46
Lithium	79	84	86
Barium	94	90	110
Sodium	180	220	200
Potassium	41	41	43
Rubidium	50	39	59

Mechanism of CO Disproportionation Promotion

This study has shown that the lithium-, sodium-, and barium-modified catalysts promote Eq. (2) relative to the other modified and unmodified catalysts and that this tendency was not due to particle size or

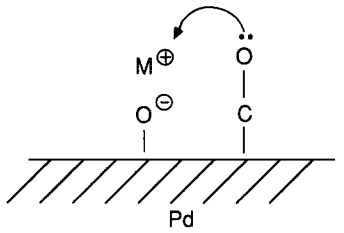

FIG. 8. Proposed mechanism by which an alkali modifier may weaken the C–O bond of an adsorbed CO molecule on an alumina-supported Pd catalyst.

support acidity. If the alkali modifiers migrate onto the surface of the active metal, an interaction between the positively charged modifier and the oxygen of an adsorbed CO molecular may occur as is shown schematically in Fig. 8. This interaction, which has been proposed by others (*22, 23, 32, 33*), weakens the carbon–oxygen bond in the CO molecule and thus facilitates its dissociation.

It follows that the strength of the C–O bond should be decreased to a greater extent by stronger interactions between the oxygen electrons in an adsorbed CO molecule and the basic modifier. The data presented here therefore imply that the lithium-, sodium-, and barium-modified catalysts have a stronger modifier–CO interaction than the other modified catalysts. The fact that the lithium and sodium modifiers are the smallest of the alkali modifiers suggests that the size or charge density of each modifier may be an important factor in the promotion of the CO disproportionation reaction.

If charge density is defined as (charge/ionic volume) (*34*), the value of charge density for each modifier can be calculated. These decrease in the following order: $Li^+ > La^{3+} > Na^+ > Ba^{2+} > K^+ > Rb^+ > C^+s$. This calculation shows that, with the exception of the La^{3+} ion, the highest charge density modifiers, Li^+, Na^+, and Ba^{2+}, are found on the catalysts which promote Eq. (2) relative to the other modified catalysts (see Figs. 4 and 5 and Table 3) and which also deactivate substantially during methanol decomposition experiments (see Table 1). In addition, the lithium-modified catalyst showed the greatest deactivation during methanol decomposition testing and the Li^+ ion also has the highest charge density of the modifiers used in this study. By contrast, the catalysts modified with the lowest charge density modifiers, K^+, Rb^+, and Cs^+, do not promote the CO disproportionation reaction and also do not deactivate significantly during methanol decomposition experiments. These results suggest that the charge density of the modifier has a significant bearing on the ability of the catalyst to promote Eq. (2).

A well known example of the effects of the variations in charge density of the Group IA elements on electrostatic or ionic interactions is found when these elements are dissolved in water. Although the ionic radii of these elements increase as the atomic number increases, the lithium ion has the largest hydration sphere of this group and the size of the hydration spheres decrease with increasing atomic number (*35*). This is due to the stronger interactions between the higher charge density positive ions and the oxygen atoms of the surrounding water molecules. Thus, when the elements with the higher charge densities, Li^+, Na^+, and Ba^{2+}, are used as catalyst modifiers, the more concentrated positive charge may interact more strongly with the oxygen atom of an adsorbed CO and serve to weaken the C–O bond and promote Eq. (2) relative to the lower charge density ions.

Figure 9 shows the relation between the activity ratio of the modified catalyst (data from Table 1) and the charge density of the respective catalyst modifier. This figure suggests that there is a relation between charge density and catalyst deactivation. The La^{3+} ion, the data point in the upper right of Fig. 9, is the single exception. Although it has a relatively high charge density, it does not deactivate at 500°C during the methanol decomposition reaction. The reason for this discrepancy is not clear although it has been suggested that La_2O_3 may be reduced by treatment with H_2 (*36*). A reduction of the La^{3+} ion would lower the charge density,

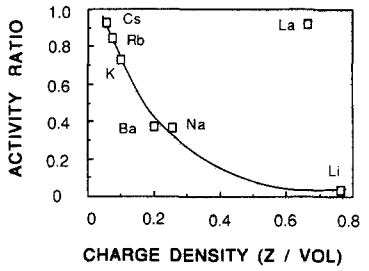

FIG. 9. Plot of activity ratio from methanol decomposition testing versus the charge density of the modifier ion.

which would improve its fit to the model. Further investigation is needed in order to understand this apparent exception.

CONCLUSIONS

The results of this investigation show that the modifier has a significant role in the deactivation of alumina-supported palladium catalysts when they are exposed to methanol at temperatures in excess of 400°C. XPS data and the ability of reoxidation to restore lost activity suggest that coking is the cause of the deactivation of the lithium-modified catalyst. No significant carbon accumulation was observed on the lanthanum-modified catalyst. In addition, the CO TPD results showed that the modifiers used in this study have a substantial effect upon the tendency of the alumina-supported palladium catalysts to promote Eq. (2). The lithium-, sodium-, and barium-modified catalysts promote Eq. (2) relative to the potassium-, rubidium-, cesium-, and lanthanum-modified and the unmodified catalysts. Moreover, there is a good correlation between the degree to which the catalysts promote Eq. (2) and the degree to which the catalysts deactivate during methanol decomposition testing. This suggests that coking is also the cause of deactivation for the sodium- and barium-modified catalysts. No correlation was observed between degree of CO disproportionation and either support acidity and particle size. Finally, a model consisting of a direct interaction between the catalyst modifier and adsorbed CO, incorporating the charge density of the modifier as the factor that determines the degree to which the modifier promotes Eq. (2), gives good agreement with the observed results.

REFERENCES

1. Finegold, J., Glinsky, G. P., and Voecks, G. E., SERI/TR-235-2083 (1984).
2. Karpuk, M. E., Dippo, J., and Ratcliff, M., SERI/TR-234-2980 (1986).
3. Masuda, K., U.S. Patent #4,499205 (1985).
4. Yoon, H., Stouffer, M. R., Dudt, P. J., Burke, F. P., and Curran, G. P., *Energy Prog.* **5** (2), 78 (1985).
5. Cowley, S. W., and Gebhard, S. C., *Colo. Sch. Mines Q.* (1983).
6. Logsdon, B. W., Gebhard, S. C., Wickham, D. T., Rutland, N. A., and Cowley, S. W., submitted for publication.
7. Wickham, D. T., Logsdon, B. W., and Cowley, S. W., *Prepr. Pap. Amer. Chem. Soc. Div. Fuel Chem.* **31,** 124 (1986).
8. Lee, J., Hanrahan, C. P., Arias, J., Martin, R. M., and Metiu, H., *Phys. Rev. Lett.* **51,** 1803 (1983).
9. Berko, A., and Solymosi, F., *Surf. Sci.* **171,** L498 (1986).
10. Crowell, J. E., and Somorjai, G. A., *Appl. Surf. Sci.* **19,** 73 (1984).
11. Rieck, J. S., and Bell, A. T., *J. Catal.* **96,** 88 (1985).
12. Blyholder, G., *J. Vac. Sci. Technol.* **11,** 865 (1974).
13. Rieck, J. S., and Bell, A. T., *J. Catal.* **99,** 262 (1986).
14. Rieck, J. S., and Bell, A. T., *J. Catal.* **99,** 278 (1986).
15. Bracey, J. D., and Burch, R., *J. Catal.* **86,** 384 (1984).
16. Sachtler, W. M. H., Shriver, D. F., Holenberg, W. B., and Lang, A. F., *J. Catal.* **92,** 429 (1985).
17. Lang, N. D., Holloway, S., and Norskov, J. K., *Surf. Sci.* **150,** 24 (1985).
18. D. Briggs and M. P. Seah (Eds.), "Practical Surface Analysis by Auger and X-ray Photo-electron Spectroscopy," New York, 1983.
19. Fleisch, T., Hicks, R. F., and Bell, A. T., *J. Catal.* **87,** 398 (1984).
20. Benson, J. E., Hwang, H. S., and Boudart, M., *J. Catal.* **30,** 146 (1973).
21. Novicki, R. S., *J. Vac. Sci. Technol.* **14** (1), 127 (1977).
22. Rieck, J. S., and Bell, A. T., *J. Catal.* **99,** 278 (1986).
23. Rieck, J. S., and Bell, A. T., *J. Catal.* **100,** 305 (1986).

24. Falconer, J. L., and Schwarz, J. A., *Catal. Rev.—Sci. Eng.* **25** (2), 141 (1983).
25. Wang, S.-Y., Moon, S. H., and Vannice, M. A., *J. Catal.* **71,** 167 (1981).
26. Fajula, F., Anthony, R. G., and Lunsford, J. H., *J. Catal.* **73,** 237 (1982).
27. Yori, J. C., Luy, J. C., Parera, J. M., *Appl. Catal.* **41,** 1 (1988).
28. Adamiec, J., Fiedorow, R. M. J., and Wonke, S. E., *J. Catal.* **95,** 492 (1985).
29. Wickham, D. T., and Cowley, S. W., to be submitted.
30. Ichikawa, S., Poppa, H., and Boudart, M., *J. Catal.* **91,** 1 (1985).
31. Rieck, J. S., and Bell, A. T., *J. Catal.* **103,** 46 (1987).
32. Rieck, J. S., and Bell, A. T., *J. Catal.* **96,** 88 (1986).
33. Bracey, J. D., and Burch, R., *J. Catal.* **86,** 384 (1984).
34. Huheey, J. E., "Inorganic Chemistry, Principles of Structure and Reactivity," 2nd ed., Harper & Row, New York, 1978.
35. Cotton, F. A., and Wilkinson, G., "Advanced Inorganic Chemistry," 4th ed., Wiley, New York, 1980.
36. Fleisch, T. H., Hicks, R. F., and Bell, A. T., *J. Catal.* **87,** 398 (1984).